PULSATIONS AT THE ONSET OF THE GREAT SOLAR BURST OF 22 OCTOBER 1989

V. S. MAKHMUTOV[1,*], J. E. R. COSTA[1,†], J.-P. RAULIN[1], P. KAUFMANN[1], P.R. LAGROTTA[1], C.G. GIMÉNEZ DE CASTRO[1], A. MAGUN[2] and K. ARZNER[2]
[1]*NUCATE and CRAAE-Centro de Rádio Astronomia e Aplicações Espaciais (Joint Center between USP, INPE, Mackenzie, UNICAMP), Universidade Estadual de Campinas, Cidade Universitária, 13083–592 Campinas, SP, Brazil*
[2]*Institute of Applied Physics, Division of Solar Observations, University of Bern, Sidlestrasse 5, CH-3012, Switzerland*

(Received 15 May 1997; accepted 19 August 1997)

Abstract. The onset phase of the 22 October 1989 great solar burst was observed at 48 GHz using the multiple beam technique, which allows unambiguous flux determination irrespective of spatial angular position changes in time. We found strong quasi-periodic pulsating structures as the flux started to rise. Two significantly different time scales of $\sim$2.5−4.5 s and $\sim$0.2−0.5 s have been observed. These pulsations might be related to magnetohydrodynamic perturbations in the active region. However the fast component also might be a signature of the acceleration and/or injection of energetic electrons.

1. Introduction

A multi-feed array was installed at the focus of the 13.7 m Cassegrain antenna at Itapetinga (Brazil) to determine angular positions of burst time structures at 48 GHz. The array produces five partially overlapping beams with half power widths of 2 arc min, displaced from each other by approximately 2 arc min. Under favourable conditions this technique can provide a spatial accuracy of a few arc sec in the determination of the emission centroid position of mm-wave bursts with a time resolution of 1 ms. The multi-feed array and the multi-beam methods used to determine source positions were described elsewhere (Georges *et al.*, 1989; Herrmann *et al.*, 1992; Costa *et al.*, 1995). Improved methods for instantaneous source size and position determinations were developed recently (Gimenez de Castro *et al.*, 1997). It is important to remember that the multiple beam technique has the advantage to determine flux from point sources, irrespective of the antenna, or source position, or movements with respect to each other. The great burst of 22 October 1989 (start time $\sim$17:38 UT) saturated all five receiver channels 5 min after the burst onset. Along the onset, the multiple beam data proved to be essential to confirm the solar origin of the pulsating phenomena at the beginning of the event.

[*]P.N. Lebedev Physical Institute RAS, Leninsky Prospect 53, 117924 Moscow, Russia.
[†]CRAAE – INPE, Sao Paulo, SP Brazil.

Solar Physics **178:** 393–403, 1998.

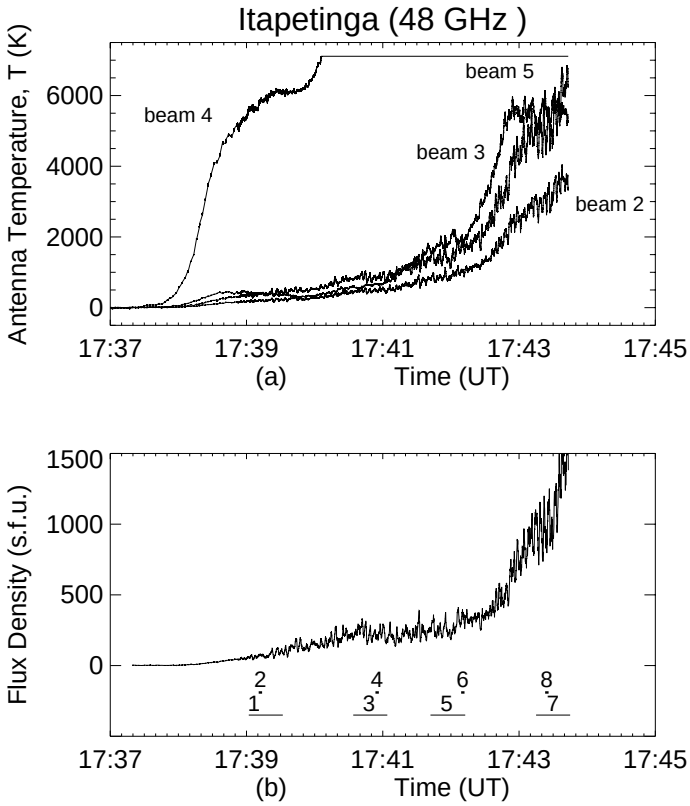

Figure 1. (a) Temporal evolution of antenna temperatures due to the radio emission at 48 GHz during the onset phase of the solar burst of 22 October 1989, as recorded by four beams of the Itapetinga antenna (beam 2, 3, 4 and 5; integration time 32 ms). (b) Flux density determined from the system of Equations (2). The horizontal bars labeled by numbers 1 to 8 indicate the time intervals for which fine time structures are shown in Figure 2.

2. Observational Results

The solar particle event of 22 October 1989 (Shea and Smart, 1990) was associated with a complex solar event originating in active region NOAA 5747, located at S27 W33 (*Solar-Geophysical Data*, 1989; hereafter *SGD*). Hα flaring emission occurred during 17:32–21:11 UT. The flare was classified as 2B/X1.5 in the optical and soft X-ray domains (*SGD*). Large radio fluxes at frequencies from a few hundred MHz to a few tens of GHz were observed during the main phase of the event ($\sim$17:57–18:10 UT). Metric type III bursts, indicating the appearance of energetic electrons in open magnetic field structures, started at about 17:43–17:44 UT. Later on, type II and IV bursts were reported during the time intervals 17:45–17:59 UT and 17:44–18:42 UT, respectively.

The burst emission at 48 GHz (Itapetinga radio telescope) started at $\sim$17:38 UT and was observable until 19:30 UT, but all channels saturated from 17:44–18:35 UT.

However, in this paper only the onset phase is of interest. Figure 1(a) shows the temporal evolution of the radio emission at 48 GHz, expressed in excess antenna temperatures, as recorded by four beams of the Itapetinga antenna (beams 2, 3, 4, and 5), with an integration time of 32 ms. Each half-power beam width (HPBW) was of 1.9 ± 0.1 arc min (Herrmann *et al.*, 1992). We mention here that the high time resolution data were not available before 17:38:52 UT.

The instantaneous antenna temperature observed by each beam i can be expressed as (Kraus, 1966)

$$T_{A,i}(\Omega) = \frac{A_e}{2k} \iint\limits_{\Omega_s} B(\Omega) P_i(\Omega)\, \mathrm{d}\Omega\ , \tag{1}$$

where $i = 1, 2, 3, \ldots$, Ω_s is the radio source extension, $B(\Omega)$ is the brightness subtended by the solid angle Ω, $P_i(\Omega)$ is the beam pattern i, A_e is the effective aperture of the antenna and k is the Boltzmann constant. For identical gaussian beams and for a point source, Equation (1) reduces to

$$T_{A,i} = \frac{A_e}{2k} S \exp\left(- \frac{[(x - x_i)^2 + (y - y_i)^2]}{2\sigma^2} \right)\ , \tag{2}$$

where S is the flux density of the source, x_i and y_i are the beam i angular positions while tracking the source, x and y are the source position in the same angular reference frame, $1/2\sigma^2 = -\ln(0.5)/(\mathrm{HPBW}/2)^2$. It is important to stress that for a point source, and solving the system of Equations (2) for three or more beams, S is an absolute determination, i.e., at each instant S is determined unequivocally, irrespective of the antenna or source position with respect to each other. Then, any time variation of S, cannot be attributed to any oscillation of the antenna and/or source position. The time profile of S derived from the system of Equations (2), using HPBW $= 1.9$, is shown in Figure 1(b). The horizontal bars labeled 1 to 8 (in Figure 1(b)) indicate the time intervals which will be shown in detail in Figure 2. These intervals were sampled as typical examples of pulsations that have been observed during the whole onset phase of the flare.

In order to describe the temporal characteristics of the burst fluctuations, S was averaged over each time interval and its average $\langle S \rangle$ subtracted from the unsmoothed time profile. The resulting differences ΔS divided by $\langle S \rangle$ are shown as a function of time in Figure 2. Two distinct and different time scales are noticeable. The corresponding pulsations are shown in the left and right columns of Figure 2, where also the mean periodicities can be measured. They lie typically in the range of $\sim$0.2–0.5 s (fast, at the right side) and $\sim$2.5–4.5 s (slow, at the left side). In terms of flux variations, both fast and slow fluctuations have relative amplitudes well above the experimental uncertainties, which are less than 1%. It is interesting to note that the fast time variations always occurred simultaneously and were superimposed on the slow time component.

In Figures 3(a) and 3(b) we show the NSO magnetogram of active region NOAA 5747, for which we have computed the extrapolated magnetic field lines

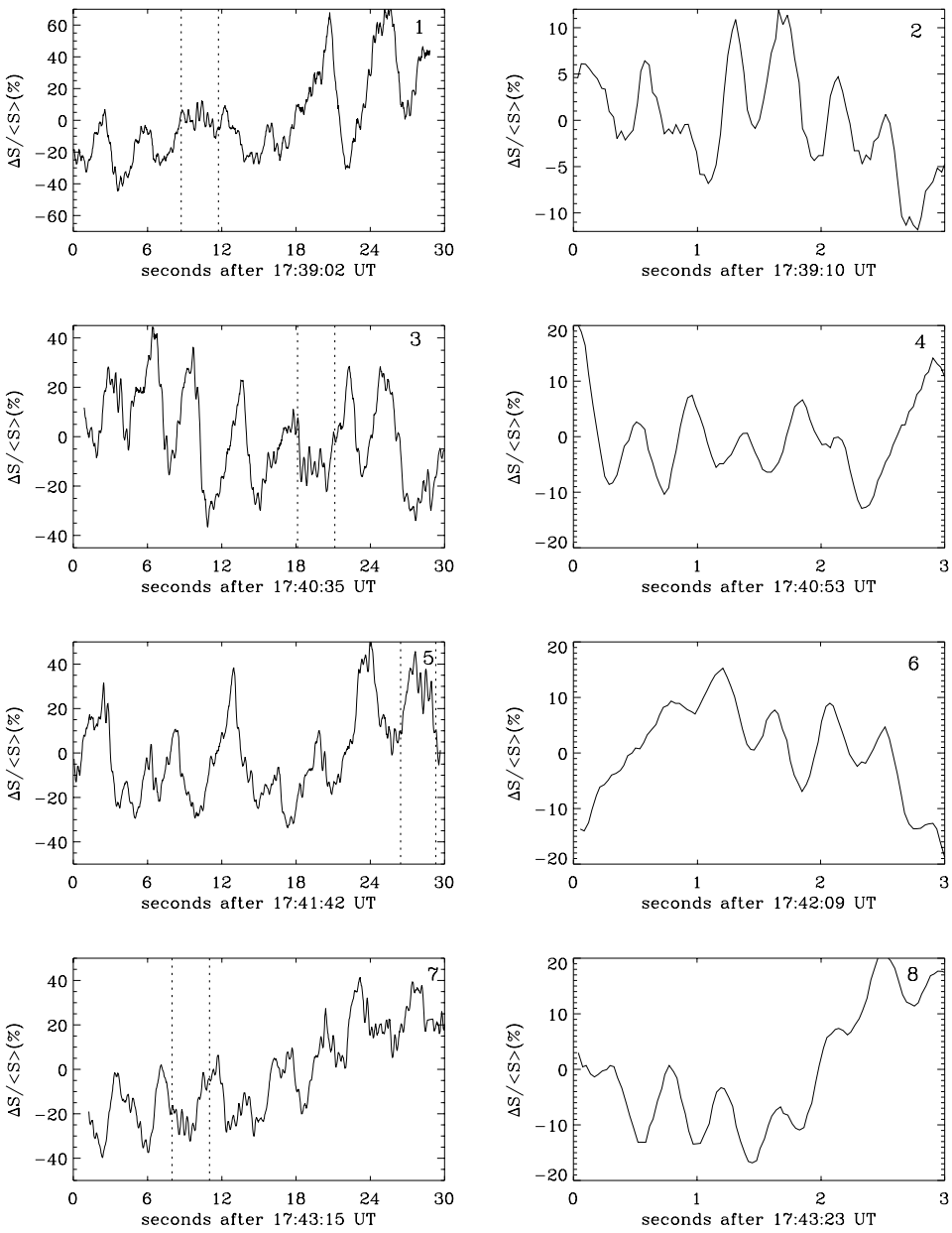

Figure 2. $\Delta S/\langle S\rangle$ evaluated during sample intervals of 30 s (left) and of 3 s (right). ΔS correspond to the flux variations relative to the mean value $\langle S\rangle$ for each selected time interval. The numbers 1 to 8 correspond to the horizontal bars labeled in Figure 1(b). The dotted vertical lines (left) represent time intervals of 3 s which are expanded in the right column plots.

using Sakurai's code (Sakurai, 1982). The extrapolation of the photospheric magnetic field assumes a potential field. A and B denote regions of strong opposite magnetic fields. The sample of dashed circles (HPBW) show the approximate location of the Itapetinga beams over the active region. The cross represents the evaluated position of the radio burst emission at 48 GHz, averaged from 17:38:50 –17:43:40 UT, and the bars have the HPBW size which represent an approximate absolute position uncertainty. The extrapolated field lines give a simplified view of the active region magnetic structure. When comparing with the location of the radio burst, there is a suggestion that the radio emission at 48 GHz might have occurred in the complex of magnetic loops connecting points A and B, near strong gradients of the magnetic field. The typical loop length given by the distance between A and B is on the order of $(0.8–9) \times 10^9$ cm.

3. Suppression of Observational Effects on Flux Determination

We can immediately discard effects caused by periodic changes in the antenna beam direction with respect to a fixed burst source or oscillations in the source position with respect to a stable antenna beam because, as already explained in the observations section, S is an absolute magnitude, determined unambiguously and does not depend on any antenna and/or source position oscillations. This is of course not true for the antenna temperature time profiles observed with different beams ($T_{A,i}$, $i = 1, 2, 3$). In this case possible antenna and/or source position oscillations will result in independent antenna temperature time profiles. In order to illustrate what was stated above, we have taken the time interval 8, bottom of the right side of Figure 2, and show the measured antenna temperature for three beams at the top of Figure 4 (a). The units are now variations of the excess antenna temperature ΔT over the mean value in that interval $\langle T \rangle$. We can see that all three time profiles are quite well correlated, or nearly 'in phase'. We have simulated the effects of ± 3 arc sec antenna oscillations (corresponding to the peak-to-peak tracking accuracy of the Itapetinga antenna) on a point source emitting a steady flux at the position calculated for the 22 October 1989 event shown in Figure 3(a). The result of this simulation is shown in Figure 4(b), where we can notice that effects of oscillations (antenna and/or source position) leads to uncorrelated signals contrary to what has been observed (Figure 4(a)). The example is meaningful and reminds us that the determination of the flux density of a point source, using the multi-beam technique have the unique advantage of suppressing any effects due to antenna and/or source position oscillations.

Other possible effects that might be considered are variations in the atmospheric water vapour, which produce changes in the absorption and direction of incoming waves. These effects are known to be considerably smaller in clear-sky conditions (see a review by Stephansen, 1981). Observations of the 22 October 1989 event were carried under clear-sky conditions. Studies of anomalous refraction at 23 GHz

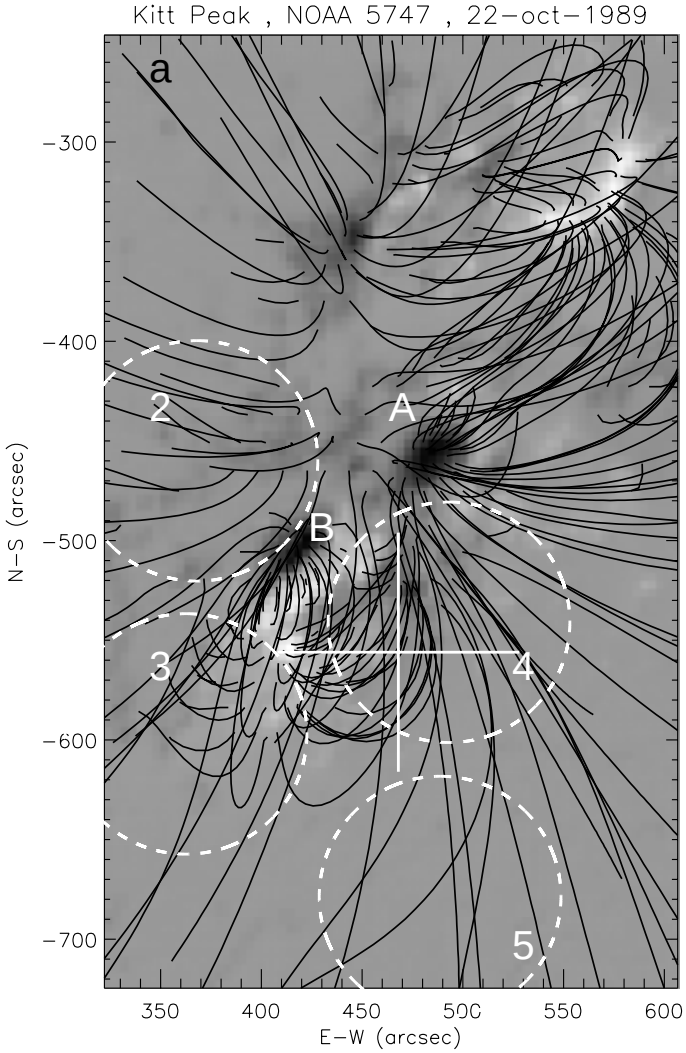

Figure 3a.

made by Altenhoff *et al.* (1987) using the 100-m Effelsberg antenna in Germany have shown that on cloudy days the 'radio-seeing' fluctuations could be as large as tens of arc sec, on time scales of several to tens of seconds. On clear days these effects became negligible. No second-subsecond 'seeing' fluctuations were reported. Careful studies were done using the Itapetinga 13.7-m antenna at 22, 44, 48, and 94 GHz (for example, Kaufmann, Strauss, and Schaal, 1982; Kaufmann *et al.*, 1984; Zodi, Kaufmann, and Zirin, 1984; Costa *et al.*, 1995). The technique, based on the tracking of the solar limb with a single beam, is sensitive to the detection of very small changes of antenna temperatures. At 48 GHz the 3σ level

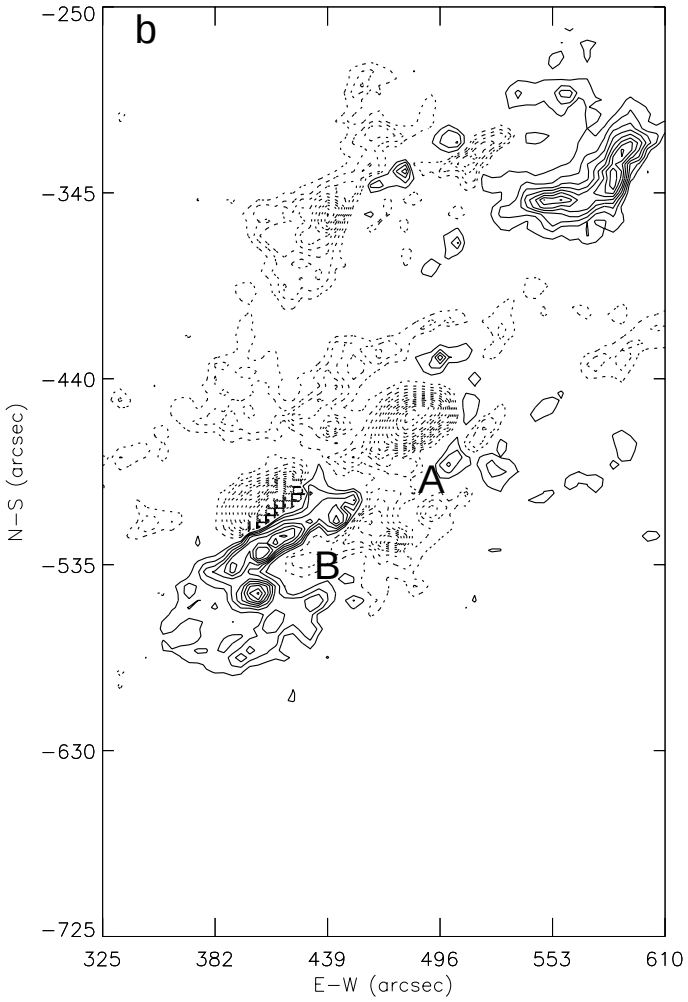

Figure 3b.

Figure 3a–b. (a) NSO magnetogram of the active region NOAA 5747 at ∼ 17:37 UT. A and B indicate the regions of strong magnetic field. Computed potential magnetic field lines are also shown. The projections of the four beams of Itapetinga antenna are shown as dashed circles. The estimated position of the radio emission source at 48 GHz is indicated with a cross, whose size indicates an approximate absolute position uncertainty. (b) Contour plot of the longitudinal photospheric magnetic field. Solid and dashed curves represent the regions of the positive and negative polarities that lie in the range of −1400 to +1000 G.

corresponds to about 6 K for a 1 ms time constant. That level is equivalent to fluctuations in the direction of incoming radiation of the order of 1 arc sec. It was found that the presence of clouds produce erratic fluctuations in time scales larger than seconds, but no fluctuations are found during clear-sky conditions. No second-subsecond fluctuations were found for any sky conditions. But again, for any

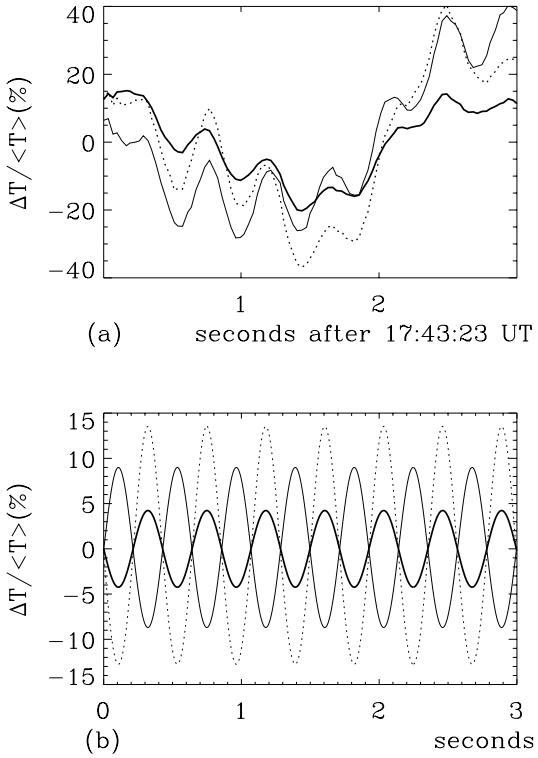

Figure 4. (a) Example of one set of antenna temperatures measured by three beams (Figure 1(b), interval 8, flux shown in Figure 2, right column) showing that the rapid fluctuations are well correlated in time. (b) Simulation of antenna beam displacements by ±3 arc sec for a constant flux point source located at the same burst position, shown in Figure 3(a). One of the beams outputs is clearly 'out of phase', contrary to the observations above.

cause producing angular variations of incoming radiation, the flux determinations using three or more beams are independent, and these causes can be similarly discarded. The presence of atmospheric density inhomogeneities in front of the antenna beams might produce variations in antenna temperature which, as said before, are negligible under clear-sky conditions. However, the observed 'in phase' antenna temperature changes in all beams shall require inhomogeneities moving across them almost simultaneously or, alternatively to have them standing in front of all beams, but with their densities varying with time. These situations are entirely unlikely. Finally, for the smaller scale sizes usually attributed to the inhomogeneous cells, of about 300 m, located at tropospheric heights of 5–10 km, subsecond time structure should require movements of the cells in front of the antenna beams at unrealistic velocities.

Therefore we can discard any instrumental or atmospheric origin for the phenomena and conclude that the observed fast and slow pulsations are genuine solar phenomena.

4. Discussion

Temporal fluctuations in solar bursts with millisecond to second time scale ranges have been reported over the whole electromagnetic spectrum. Metric to decimetric fast (less than 1 s) time structures (Dröge, 1961; Slottje, 1978; Benz, 1994; Aschwanden *et al.*, 1994) are usually narrowband and attributed to coherent emission. They may also be a response to pulsed particle accelerations. At hard X-rays, second to sub-second time structures were suggested as evidence for discrete bursts (elementary flare burst), building up larger events (Frost, 1969; van Beek, De Feiter, and de Jager, 1974; Kiplinger, Frost, and Orwig, 1983; Hurley *et al.*, 1983; Vilmer *et al.*, 1994, Fleishman, Stepanov, and Yorovsky, 1994). At cm−mm waves, sub-second time structures were attributed to discrete injections of high-energy electrons (Kaufmann, Piazza, and Raffaelli, 1977; Kaufmann *et al.*, 1980), and time pulsations on the scale of seconds were associated with magnetohydrodynamic disturbances (Zodi, Kaufmann, and Zirin, 1984).

In the present study we have found superimposed quasi-periodic fluctuations in the 48 GHz radio emission during the onset phase of a great solar flare, with time scales in the ranges of $\sim 0.2-0.5$ s and $\sim 2.5-4.5$ s. It is important to note that the variations were observed from the beginning of the event, and that they are most likely to be intrinsic to the source. They are too short to be related to the lifetime of the emitting electrons under the influence of collisions with ambient electrons (tens of seconds for densities $\sim 10^{10}$ cm^{-3} and electron energies of a few hundreds of keV). We suggest that the slow time variations (~ 3 s) were caused by MHD disturbances propagating along the loops connecting A with B with Alfvén speed, thereby modulating the magnetic field in the 48 GHz source region, as well as its direction with respect to the observer. In particular, changes by 20 deg of the viewing angle between $\mathbf{B}$ and the observer can result in a modulation of the gyrosynchrotron emission up to 60% (Dulk, 1985). For typical values of B $\sim 400-700$ G and densities between $N_e \approx 10^9-10^{10}$ cm^{-3} in the source region, we find that the travel time of such disturbances is in the range 1.5−3 s, when the estimated loop length $L \approx (0.8-9) \times 10^9$ cm is taken into account. The magnetic field value is a lower limit because it is probably more complicated than that shown in Figure 3(a), and might also include the twist of the field lines. As for the fast component ($\sim 0.2-0.5$ s), we suggest that they are probably the signature of acceleration and/or injection of energetic electrons. However, we cannot exclude the possibility that they may be caused by MHD wave disturbances in smaller magnetic loops.

In small to moderate bursts, fluctuations in the mm-emission occur typically after the onset of the impulsive phase (Kaufmann, Strauss, and Schaal, 1982; Zodi, Kaufmann, and Zirin, 1984; Correia *et al.*, 1995). The fluctuations observed during the energetic event studied here occurred already at the beginning of the impulsive phase. Therefore they might be representative of peculiar processes occurring only in large flares.

5. Conclusions

We have analyzed the temporal peculiarities of the radio burst emission recorded by the Itapetinga telescope at 48 GHz during the onset phase of the great solar burst of 22 October 1989. The multiple beam technique offers the unique possibility to determine fluxes unequivocally, suppressing effects due to observations. We have found quasi-periodic fluctuations with periods in the range of $\sim 0.2-0.5$ and $\sim 2.5-4.5$ s. They occurred right from the start of the event and lasted during the observable part of the onset phase. Fast and slow pulsations found in the mm-λ range are usually observed some time after the onset of emission (Kaufmann, Strauss, and Schaal, 1982; Zodi, Kaufmann, and Zirin, 1984; Correia *et al.*, 1995). In that sense the very early onset of the observed pulsations is unique and may be characteristic for large flares. We have suggested that the slower quasi-periodic time variations ($\sim$ 3 s), may be related to the propagation of MHD disturbances along coronal magnetic loops. The fast pulsations probably are the signature of acceleration and /or injection of energetic electrons. However, they also may be caused by the propagating MHD disturbances in smaller magnetic loops.

Acknowledgements

We would like to thank Dr Detrick Branston for the NSO magnetogram. VSM and JPR would like to thank the Fundação de Amparo à Pesquisa do Estado de São Paulo (FAPESP, Brasil) for financial support through contracts Nos. 94/5957−9 and 96/06956−1, respectively. PRL and CGGC would like to thank the Conselho Nacional de Desenvolvimento Científico e Tecnológico (CNPq, Brasil), for financial support through contracts Nos. 552353/94−0, 150087/96−9, respectively. AM and KA would like to thank the Swiss National Science Foundation for financial support through grant No. 2000−042265.94

References

Altenhoff, W. J., Baars, J. W. M., Downes, T., and Wink, J. E.: 1987, *Astron. Astrophys.* **184**, 381.
Aschwanden, M. J., Benz, A. O., Dennis, B. R., and Kundu, M. R.: 1994, *Astrophys. J. Suppl.* **90**, 631.
Benz, A. O.: 1994, *Space Sci. Rev.* **68**, 135.
Correia, E., Costa, J. E. R., Kaufmann, P., Magun, A., and Herrmann, R.: 1995, *Solar Phys.* **159**, 143.
Costa, J. E. R., Correia, E., Kaufmann, P., Magun, A., and Herrmann, R.: 1995, *Solar Phys.* **159**, 157.
Dröge, F.: 1961, *Inf. Bull. Solar Radio Obs.* No. 8.
Dulk, G. A.: 1985, *Ann. Rev. Astron. Astrophys.* **23**, 169.
Fleishman, G. D., Stepanov, A. V., and Yorovsky, Yu. F.: 1994, *Space Sci. Rev.* **89**, 205.
Frost, K. J.: 1969, *Astrophys. J.* **158**, L159.
Georges, C. B., Schaal, R. E., Costa, J. E. R., Kaufmann, P., and Magun, A.: 1989, *Proc. 2nd Int. Microwave Sympos., Rio de Janeiro)*, p. 447.
Gimenez de Castro, C. G., Raulin, J.-P., Makhmutov, V. S., Kaufmann, P., Costa, J. E. R., and Magun, A.: 1997, in preparation.

Herrmann, R., Magun, A., Costa, J. E. R., Correia, E., and Kaufmann, P.: 1992, *Solar Phys.* **142**, 157.
Hurley, K., Niel, M., Talon, R., Estulin, I. V., and Dolidze, V. C.: 1983, *Astrophys. J.* **265**, 1076.
Kaufmann, P., Piazza, L. R., and Raffaelli, J. C.: 1977, *Solar Phys.* **54**, 197.
Kaufmann, P., Strauss, F. M., and Schaal, R. E.: 1982, *Solar Phys.* **78**, 389.
Kaufmann, P., Strauss, F. M., Opher, R., and Laporte, C.: 1980, *Astron. Astrophys.* **87**, 58.
Kaufmann, P., Correia, E., Costa, J. E. R., Dennis, B. R., Hurford, G. J., and Brown, J. C.: 1984, *Solar Phys.* **91**, 359.
Kiplinger, A., Frost, K. J., and Orwig, L. E.: 1983, *Solar Phys.* **84**, 311.
Kraus, J. D.: 1966, *Radio Astronomy*, McGraw-Hill Book Co., New York.
Sakurai, T.: 1982, *Solar Phys.* **76**, 301.
Shea, M. A. and Smart, D. F.: 1990, *Solar Phys.* **127**, 297.
Slottje, C.: 1978, *Nature* **275**, 520.
Solar Geophysical Data: 1989–1990, NOAA, Boulder.
Stephansen, E. T.: 1982, *Radio Sci.* **16**, 609.
van Beek, H. F., De Feiter, L. D., and de Jager, C.: 1974, *Space Res.* **14**, 447.
Vilmer, N., Trottet, G., Barat, C., Dezalay, J. P., Talon, R., Sunyaev, R., Terekhov, O., and Kuznetsov, A.: 1994, *Solar Phys.* **68**, 233.
Zodi Vaz, A. M., Kaufmann, P., and Zirin, H.: 1984, *Solar Phys.* **92**, 283.